ACS APPLIED MATERIALS & INTERFACES

Research Article

www.acsami.org

Role of Additives in Composite PEI/Oxide CO_2 Adsorbents: Enhancement in the Amine Efficiency of Supported PEI by PEG in CO_2 Capture from Simulated Ambient Air

Miles A. Sakwa-Novak,[†] Shuai Tan,[†] and Christopher W. Jones*[,†]

[†]School of Chemical & Biomolecular Engineering, Georgia Institute of Technology, 311 Ferst Dr., NW, Atlanta, Georgia 30332, United States

Supporting Information

ABSTRACT: Supported amines are promising candidate adsorbents for the removal of CO_2 from flue gases and directly from ambient air. The incorporation of additives into polymeric amines such as poly(ethylenimine) (PEI) supported on mesoporous oxides is an effective strategy to improve the performance of the materials. Here, several practical aspects of this strategy are addressed with regards to direct air capture. The influence of three additives (CTAB, PEG200, PEG1000) was systematically explored under dry simulated air capture conditions (400 ppm of CO_2, 30 °C). With SBA-15 as a model support for poly(ethylenimine) (PEI), the nature of the additive induced heterogeneities in the deposition of organic on the interior and exterior of the particles, an important consideration for future scale up to practical systems. The PEG200 additive increased the observed thermodynamic performance (~60% increase in amine efficiency) of the adsorbents regardless of the PEI content, while the other molecules had less positive effects. A threshold PEG200/PEI value was identified at which the diffusional limitations of CO_2 within the materials were nearly eliminated. The threshold PEG/PEI ratio may have physical origin in the interactions between PEI and PEG, as the optimal ratio corresponded to nearly equimolar OH/reactive (1°, 2°) amine ratios. The strategy is shown to be robust to the characteristics of the host support, as PEG200 improved the amine efficiency of PEI when supported on two varieties of mesoporous γ-alumina with PEI.

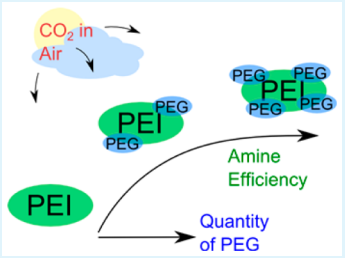

KEYWORDS: *CO_2 capture, air capture, supported amines adsorbents, poly(ethyleninime), poly(ethylene glycol), mesoporous materials*

INTRODUCTION

As global CO_2 concentrations continue to rise as a result of emissions from anthropogenic activity, the development of clean technologies to produce energy and reduce such emissions has become urgent.[1−3] Toward this end, the removal of CO_2 from the emissions mixture of power plants is necessary if cheap and abundant fossil fuels continue to be used to produce electricity on a global scale.[4−6] In addition, the removal of CO_2 directly from ambient air has gained attention as a strategy that would be part of an emissions reduction paradigm accounting for highly dispersed emissions that result from the transportation, industrial and residential sectors of the economy, and theoretically allowing for "negative emissions" if widely adopted.[7−13] However, for CO_2 removal from flue gas or from ambient air to be realized on a relevant scale, suitable technologies must be developed that allow for efficient process operation at an acceptable cost.

Supported amine adsorbent materials are promising candidates for use in both flue gas and direct air CO_2 capture technologies.[8,14−16] These materials extrapolate the aqueous amine chemistry of absorbent solutions that are effective but costly for CO_2 removal from flue gas into solid adsorbents. These solids offer the potential of reduced regeneration energy, due to a lower heat capacity relative to the liquid amine solution, and equipment corrosion. Such materials incorporate amine functionalities into high-surface-area porous solids, which can then interact with CO_2 in a chemisorptive fashion. This results in a relatively high heat of adsorption of CO_2 with the materials,[17] resulting in steep adsorption isotherms. These steep isotherms give the materials promise in CO_2 capture from air, as significant CO_2 capacities have been demonstrated for materials under the sparingly dilute 400 ppm concentration of CO_2 in the ambient air.[18−22] It has been proposed to utilize a honeycomb monolith geometry as gas/solid contactor for air capture to facilitate the large gas flows required by the process at low pressure drop.[23,24] A preliminary techno-economic analysis exploring an amine functionalized honeycomb monolith for air capture suggested that the operating cost could be as low as ~ $100/ton CO_2, and suggested that an improvement in the adsorption capacity and reduction in heating load could lead to substantial performance improvements.[25]

The utility of amine materials is typically quantified by a number of parameters, with perhaps the most important being the "amine efficiency" of the material, defined as the moles of CO_2 adsorbed at a particular partial pressure of CO_2

Received: August 14, 2015
Accepted: October 20, 2015
Published: October 20, 2015

DOI: 10.1021/acsami.5b07545
ACS Appl. Mater. Interfaces 2015, 7, 24748−24759

normalized by the moles of amine present in the material. The maximum chemisorptive amine efficiency of a supported amine material is set by the CO_2−amine interaction chemistry, where it is suggested that two amines are required to immobilize one CO_2 by the formation of ammonium carbamate pairs in the absence of water.[26] However, amine efficiencies are typically reported to be lower than this theoretical maximum of one-half, which has been hypothesized to be associated with amines that are not in close proximity to one another in low loaded materials[27−29] or amines that are buried and subjected to CO_2 diffusional limitations in highly loaded materials.[30]

Hence, an important research focus has been to develop synthetic strategies to engineer supported amine materials to have increased amine efficiencies. One route that is effective in this regard is to incorporate non amine-containing molecules or polymers into poly(ethylenimine) (PEI) impregnated porous materials. PEI is the most frequently reported aminopolymer used for CO_2 adsorption in solids, due to its amine rich structure and commercial availability. Poly(ethylene glycol) (PEG), has been incorporated into amine containing solids and has led to improved capacities, and in some cases, kinetics.[31−36] In 2001, Satyapal et al. reported using poly(ethylene glycol) (PEG) and PEI supported on porous poly(methyl methacrylate) (PMMA) in the removal of CO_2 from air in spacecraft, though in this early work, the effect of PEG on the CO_2 capacity and amine efficiency was not directly quantified.[32] Song reported an increase in the CO_2 capacity of an MCM-41 silica impregnated with PEG and PEI at a weight ratio of 2:3 g PEG/g PEI and found that the capacity increased from 68.7 mg/g to 77.1 mg/g in adsorption using pure CO_2 at 75 °C.[33] Drage and Snape incorporated PEI and PEG onto fly ash derived carbon adsorbents and altered the PEI weight percent of the sorbents while keeping the PEG weight percent constant at 20. They reported CO_2 adsorption profiles collected at 75 °C with pure CO_2 from TGA experiments for PEG/PEI sorbents at PEI weight loadings of 20, 40, and 60% and found that the addition of PEG increased the uptake, in each case, though to a lesser extent at higher PEI loadings.[34] Olah's group has studied the effect of PEG on PEI impregnated fumed silica sorbents. In one study they reported decreases in the per gram CO_2 capacity of sorbents with PEG incorporated at a PEG/PEI ratio of 0.5, but enhanced isothermal desorption of the CO_2 from the material using vacuum.[35] In another study they reported increases in the per gram CO_2 capacity as well as the amine efficiency for mixtures of PEG and PEI supported on silica nanoparticles when the percentage of PEG in the sorbent ranged from 0 to 12.5.[36] In that work, the sorbents were prepared in a two-step process of addition of PEG followed by addition of PEI to the silica. They reported an amine efficiency as high as 62% for adsorption of pure CO_2 in a "static procedure" for the optimal material. Wang explored the incorporation of a wide range of additive molecules into PEI impregnated in hierarchical porous silica monoliths and found that all of the additives increased the CO_2 capacity of the sorbent compared to the sorbent with just PEI when adsorbing pure CO_2 at ambient pressure and varying temperatures.[37] The same group reported similar results when incorporating additive molecules into silica templated mesoporous carbons with large pore volumes.[38]

Additionally, PEG has been shown to reduce the oxidation of supported amines, suggested to be the result of hydrogen bonding between the PEG and PEI.[39−41] Similarly, improvements have been shown to result from the incorporation of a wide range of co-impregnated surfactant molecules,[37,38,42,43] including those left from the template used during silica syntheses,[44−46] as well as grafted and ungrafted silanes[20,47−51] and inorganics such as potassium carbonate.[52] A more detailed summary of these studies is provided in the Supporting Information.

Several hypotheses have been proposed to explain the additive promoting effect, including improved dispersion of impregnated PEI,[37,44] a reduction in the organic viscosity,[36] and an increase in the theoretical amine efficiency through the formation of bicarbonates.[33] Compelling evidence that the nature of the enhancement is kinetic (rather than thermodynamic) has been reported in several papers, where the optimal adsorption temperature was lower for samples with additives relative to those without additives, reflecting an effective decrease in the aforementioned diffusional resistances. However, a more fundamental description of what gives rise to these phenomena has not been compellingly elucidated. Recently, Baker et al. addressed this question directly with the hypothesis that the promoting effect of PEG was due to the Lewis basicity of the polymer, however their study did not fully validate the hypothesis.[53]

While additive molecules have generally enhanced the performance of supported polyamines, the degree of improvement has been a strong function of the experimental conditions such as material composition and adsorption temperature. In this regard, the goal of this work was to explicitly assess the effect of additive incorporation on the adsorption performance of PEI impregnated mesoporous oxides upon exposure to ultradilute, 400 ppm of CO_2. This was done to directly assess the efficacy of the strategy for improving materials for air capture processes, namely, to quantify changes in amine efficiency for materials of varied composition, such that promising compositions could be targeted for the scale up of the technology. Additionally, the use of such low pressure CO_2 ensures that CO_2 physisorption was negligible,[54] and that only the most reactive amines participate in the adsorption, thus providing an interesting experimental platform to study the underlying adsorption phenomena. Additionally, practical considerations such as pore filling, adsorption dynamics and support characteristics were studied. The effect of three additives, CTAB, PEG200, and PEG1000 were systematically co-impregnated with PEI into a model SBA-15 silica support. The best performing additive, PEG200, was subsequently studied at varying PEI loadings and on two varieties of mesoporous alumina. A kinetic threshold was reached, whereby at PEG/PEI ratios that correspond to nearly equimolar OH/reactive (1°, 2°) amine ratios, the adsorption became completely thermodynamically controlled.

EXPERIMENTAL SECTION

Preparation of Materials. *Chemicals.* All chemicals were used as purchased from the supplier. Pluronics P123, tetraethylorthosilicate (TEOS) (98%, Reagent grade), nitric acid, poly(ethylenimine) (PEI) (Mw 800, Mn 600), and poly(ethylene glycol) (av mol wt 200) were purchased from Sigma-Aldrich. Methanol (ACS grade) and hydrochloric acid (fuming, ACS grade) were purchased from BDH Chemicals. Pseudoboehmite (74.3% Al_2O_3, Capitol B) and the "commercial" γ-alumina (Sasol SBa-200) were purchased from Sasol North America. Cetyltrimethylammonium bromide (CTAB) (99+%. TLC grade) was purchased from Acros Organics. Poly(ethylene glycol) (av mol wt 1000) was purchased from J.T. Baker. Ethanol (200 proof) was purchased from Koptec.

DOI: 10.1021/acsami.5b07545
ACS Appl. Mater. Interfaces 2015, 7, 24748−24759

SBA-15 Silica. SBA-15 silica was synthesized according to the following procedure: 24 g of Pluronic P123 was dissolved in an acidic solution of 120 mL fuming (~37%) HCl and 636 g H_2O under stirring at room temperature in a 2L Erlenmeyer flask. Once the polymer template was fully dissolved, 46.26 g of TEOS was dropwise added to the mixture by pipet. This solution was vigorously stirred at 40 °C for 20 h, before the stir bar was removed and the synthesis mixture was hydrothermally aged at 100 °C under ambient pressure for 24 h. After aging, the material was immediately filtered and washed with copious amounts of DI H_2O, before drying at 70 °C overnight. Finally, the template was removed by calcination at 550 °C for 10 h, with a ramp rate of 2 °C/min and an intermediate H_2O removal step of 200 °C for 2 h.

Mesoporous Templated γ-Alumina. Mesoporous templated γ-alumina was prepared by a method used previously for the synthesis and preparation of γ-alumina supported amine materials[55,56] but developed elsewhere.[57−59] P123 was used as a soft template in the self-assembly of pseudoboehmite nanoparticles into a mesoporous structure. To prepare the alumina, we first peptized 13.75 g of pseudoboehmite by dispersing and sonicating it for 90 min in an acidic mixture consisting of 1.27 g nitric acid (~70%) and 200 mL DI H_2O and then allowed it to age at 60 °C for 17 h. Separately, 15.3 g P123 was dissolved in 200 mL of ethanol, and the peptized pseudoboehmite containing dispersion was slowly added to this, and the resultant mixture was stirred at room temperature for 24 h. Solvent evaporation was then performed by aging at 60 °C for 48 h in an open beaker. The resulting yellowish solid was further dried at 75 °C before being calcined in static air at 700 °C for 4 h with an intermediate drying step at 150 °C to remove water. A temperature ramp rate of 1 °C/min was used for both temperature step.

Preparation of Adsorbents. Adsorbents were prepared by impregnation of a given amount of PEI and additive into a support material in one step using methanol as a solvent. Prior to adsorbent preparation, the silica or alumina support materials were dried under vacuum (~20 mTorr) overnight at ~100 °C to remove adsorbed species. To prepare the adsorbent, we weighed 0.25 g of dried support material and dispersed it in 20 mL of methanol in a 100 mL round-bottom flask. Separately, given amounts of PEI and additive were weighed and added to a 25 mL round-bottom flask, before 10 mL of methanol was added. The two mixtures, one containing the support and the other containing the organic contents, were stirred separately for 1 h to equilibrate. Then, the solution containing PEI and additive was added by pipet to the solution containing support. This mixture was then stirred for 3 h to equilibrate. Finally, the methanol was removed by rotary evaporation at ~60 °C, and the resulting powder was further dried under high vacuum (~20 mTorr) at ~60 °C for 12−18 h before collection. Samples were stored in vials under ambient conditions prior to evaluation.

Characterization Methods. *Thermogravimetric Analysis (TGA).* TGA was used to estimate total organic compositions of adsorbents using a Netzsch STA409PG. Here, 10−14 mg of sample was heated from ambient condition to 900 °C in the presence of air and the weight loss was recorded. Total organic loadings were taken as the sample weight loss between 120 and 900 °C, and were normalized by the residual mass of the sample recorded at 900 °C. Strongly bound water and water produced via silanol or aluminol condensation was subtracted from this value by estimation from TGA analysis of the appropriate bare support.

Elemental Analysis. Atlantic Microlabs (Norcross, GA) performed elemental analyses for carbon, nitrogen, and hydrogen. Samples were dried at 100 °C under vacuum at the facility prior to analysis to ensure a dry material basis. Estimates of the ratio of additive to PEI in a given sample were derived from the obtained C/N ratio according to eq 1 (g additive/g PEI was derived explicitly as a function of the other, known or measured, quantities).

$$\frac{\mathrm{g\,C}}{\mathrm{g\,N}} = \frac{\frac{\mathrm{g\,C}}{\mathrm{g\,PEI}}\mathrm{g\,PEI} + \frac{\mathrm{g\,C}}{\mathrm{g\,additive}}\mathrm{g\,additive}}{\frac{\mathrm{g\,N}}{\mathrm{g\,PEI}}\mathrm{g\,PEI}} \quad (1)$$

Nitrogen Physisorption. Nitrogen physisorption experiments were performed on a Micromeritics Tristar II 3020 instrument at 77 K. Surface areas were estimated using the BET method, using data obtained below a partial pressure of 0.3. Pore volumes were estimated by the total N_2 sorption at a partial pressure of 0.99. Surface areas and pore volumes of composite materials (organic + inorganic) were normalized to per gram SiO_2 or Al_2O_3 using the inorganic weight percent derived from TGA experiments. Pore size distribution of the SBA-15 was estimated using the NLDFT equilibrium model with Quantachrome VersaWin software. Pore size distributions of the alumina samples were estimated using the BdB-FHH method employing the adsorption branch of the N_2 isotherms and assuming cylindrical pores. NLDFT was not used for the alumina PSD calculations due to the nature of the calculation, requiring a silica surface.

X-ray Diffraction (XRD). XRD patterns were collected using a PANalytical X'Pert diffractometer using Cu Kα radiation.

FTIR Spectroscopy. A Bruker Vertex 80v optical bench was used to collect FTIR spectra. For powder samples, ~ 1 mg of sample was mixed with ~100 mg KBr and pressed to pellets. For polymer samples, a small amount of (liquid) polymer was brushed onto a preformed KBr pellet.

X-ray Photoelectron Spectroscopy. was performed on a Thermo K-Alpha spectrometer and a monochromatic Al Kα X-ray source. Scans were taken from 0 to 1350 eV with a scanning step of 0.1 eV. The spectrum was calibrated using the C 1s peak at 284.6 eV. Vacuum pressure of 4×10^{-7} Torr was employed in the analytical chamber during analysis.

CO_2 Adsorption. CO_2 adsorption experiments were performed by thermogravimetric analysis (TGA) using a TA Instruments Q500 apparatus using 14 mg (± 1 mg) of material. Estimates of CO_2 capacities were obtained by pretreating the given sample under 90 mL of helium at 110 °C for 3 h, followed by thermal equilibration at 30 °C and subsequent exposure to a gas mixture of 400 ppm of CO_2 balanced by helium at the same temperature and gas flow rate for 12 h.

RESULTS AND DISCUSSION

An SBA-15 silica was synthesized and used as a model support to study the effect of additive mixtures on impregnated PEI during CO_2 adsorption. The N_2 physisorption profile, NLDFT pore size distribution and small angle XRD pattern of the SBA-15 are shown in Figures 1. The textural properties derived from the N_2 physisorption data are tabulated in Table 1. The NLDFT pore size distribution suggested a primary mesopore size of 8.6 nm, which corresponded well with the d_{100} spacing of ~9.2 nm derived from XRD. The surface area and pore volume of the SBA-15 were consistent with those found in the literature.

Effect of Additive Type on Amine Efficiency in SBA-15. Three additives, cetyltrimethylammonium bromide (CTAB), Mw 200 poly(ethylene glycol) (PEG200) and Mw 1000 poly(ethylene glycol) (PEG1000), were coincorporated with poly(ethylenimine) (PEI) into the SBA-15 to assess how the nature and quantity of additive changed the amine efficiency of the adsorbent at 400 ppm of CO_2. To prepare an adsorbent, specific amounts of additive and PEI were dissolved in methanol and subsequently equilibrated with an SBA-15/methanol dispersion before the methanol was removed by rotary evaporation. FTIR spectra, reported in Figure S1 of the Supporting Information, confirmed that the additives were incorporated into the resultant materials. Additional spectra of PEI and PEG physically mixed as liquids, impregnated alone, and co-impregnated into SBA-15 are provided in Figure S2 of the Supporting Information as well.

Table 1 shows the physical and textural properties of the resultant materials, as well as the CO_2 capacities measured by

DOI: 10.1021/acsami.5b07545
ACS Appl. Mater. Interfaces 2015, 7, 24748−24759

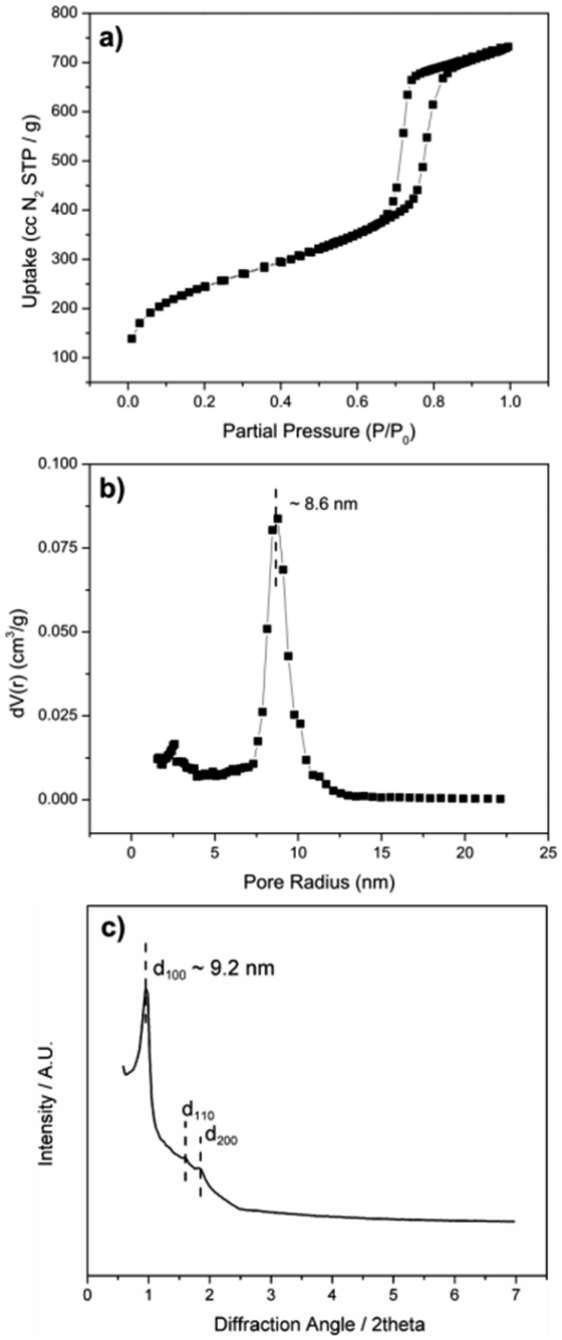

Figure 1. (a) N_2 physisorption, (b) NLDFT pore size distribution, and (c) XRD pattern of SBA-15.

TGA. Each of the materials shown in Table 1 was prepared with a constant PEI to SiO_2 ratio of ~0.45 in the preparation mixture. The slight discrepancy between this PEI to SiO_2 ratio in the preparation mixture and that reported in Table 1 for the nonadditive containing control material reported is attributed to adsorbed water on the silica and small losses of silica during sample handling, which would decrease the effective silica weight in the mixture slightly.

For each of the additives coincorporated with PEI, as the organic content increased the C/N ratio and correspondingly the additive/PEI mass ratio also increased, while the surface areas and pore volumes decreased. Because the additives were nonamine containing (with the exception of the quaternary amine in CTAB, which has a much higher C/N ratio than PEI), the amine content per gram of adsorbent decreased as the additive content increased.

The CO_2 capacities of the PEI/PEG200 and PEI/PEG1000 were higher than the reference material at low PEG/PEI content; however the CO_2 capacities of the samples decreased as the additive content increased for each additive molecule. For the PEI/PEG200 samples, as the PEG content increased, the decrease in the CO_2 capacity was less than the decrease in the amine loading, indicating that the amine efficiency increased in these materials even as the CO_2 capacity decreased. Most related studies in the literature have focused solely on changes to the CO_2 capacity, while the amine efficiency is arguably a more practically important metric. It is important to note that that the reference sample with (only) PEG200 had a negligible CO_2 uptake at the 400 ppm adsorption condition, indicating that the increased capacities of PEI/PEG200 samples were not simply a result of PEG adsorbing CO_2 independently of PEI. The amine efficiencies of each sample plotted against the estimated additive/PEI mass ratio are shown in Figure 2. The horizontal line drawn through the figure represents the amine efficiency of the reference PEI/SBA-15 material with no additive. Samples at common additive/PEI content were grouped into low, medium and high loading groups for ease in observation of later data analysis.

The incorporation of both low and high molecular weight PEG increased the amine efficiency over all of the loadings tested, while the incorporation of CTAB decreased the amine efficiency. This is contrary to the findings of Wang et al.,[37,43] who reported an increase of ~10% in the CO_2 capacity of porous silicas and carbons impregnated with PEI and 5 wt % of CTAB, and Sayari et al.[44] who reported a near doubling of the CO_2 capacity during adsorption at room temperature when PEI was impregnated in a pore expanded MCM-41 with CTAB left behind from the silica synthesis. However, in comparison to Wang's study, the materials here contained much higher amounts of CTAB and a support of differing characteristics was used, each of which may play a role in setting the extent to which the adsorption behavior is changed. In Sayari's study, where the MCM-41 support was similar in textural characteristics to the SBA-15 used (albeit with a smaller pore size), the CTAB was necessarily well dispersed on the walls of the silica, having been left from the silica synthesis. Additionally, the adsorption gas was pure CO_2 in that study, whereas here it was 400 ppm. Nonetheless, the strong difference in adsorption behavior of samples with CTAB between the two studies highlights the importance of the dispersion of CTAB on altering the adsorption behavior of impregnated PEI. The trends in Figure 2 also show that the amine efficiency decreased as the additive levels increased in the PEG1000 and CTAB incorporated samples, while the opposite was true in the PEG200 incorporated samples.

Pore Filling Characteristics. Physical differences between the materials were probed with N_2 physisorption and XPS analysis. BET surface areas and pore volumes derived from N_2 physisorption and normalized per gram SiO_2 are reported in Table 1. The percentage reduction in pore volume caused by pores being filled or blocked by organic was estimated by normalizing the N_2 physisorption isotherms per gram SiO_2, and comparing the final pore volumes of the materials with those of the unmodified SBA-15 support. Figure 3 shows this percentage reduction in pore volume plotted against the additive/PEI mass ratio for materials with all three additives at varying loading.

DOI: 10.1021/acsami.5b07545
ACS Appl. Mater. Interfaces 2015, 7, 24748−24759

Table 1. Physical, Textural, and CO_2 Adsorption Properties of SBA-15/PEI/Additive Mixtures

	organic/silica (g Org/g SiO_2)[a]	carbon/nitrogen (mol C/mol N)[b]	additive/PEI (g/g)[c]	surface area (m^2/g SiO_2)[d]	pore volume (cm^3/g SiO_2)[e]	amine content (mmol N/g)[b]	CO_2 capacity (mmol CO_2/g)	amine efficiency (mol CO_2/mol N)
Reference Materials								
bare SBA-15				880	1.13			
PEI (no PEG)	0.51	2.2		317	0.67	6.36	0.63	0.10
PEG200 (no PEI)	0.33			35	0.11		0.00	0.00
Low Molecular Weight PEG (PEG200)								
PEG200	0.54	2.6	0.31	236	0.50	5.75	0.79	0.14
PEG200-low	0.66	3.2	0.61	263	0.54	4.97	0.73	0.15
PEG200-med	1.32	5.6	1.82	147	0.33	3.88	0.64	0.16
PEG200-high	2.13	8.8	3.42	1	0.00	3.42	0.49	0.14
High Molecular Weight PEG (PEG1000)								
PEG1000-low	0.65	2.9	0.47	262	0.53	5.37	0.71	0.13
PEG1000-med	1.39	5.8	1.92	4	0.01	4.17	0.49	0.12
PEG1000-high	2.29	10.2	4.08	1	0.00	2.84	0.30	0.11
CTAB								
CTAB- low	0.60	2.8	0.32	277	0.56	5.70	0.55	0.10
CTAB- med	1.30	5.7	1.77	74	0.17	4.63	0.31	0.07
CTAB- high	1.99	8.1	3.60	47	0.12	4.03	0.21	0.05

[a]Estimated by TGA. [b]Estimated from elemental analysis. [c]Estimated from elemental analysis using eq 1. [d]Estimated with BET method from N_2 physisorption. [e]Estimated from total N_2 adsorbed at P/P_0 = 0.99.

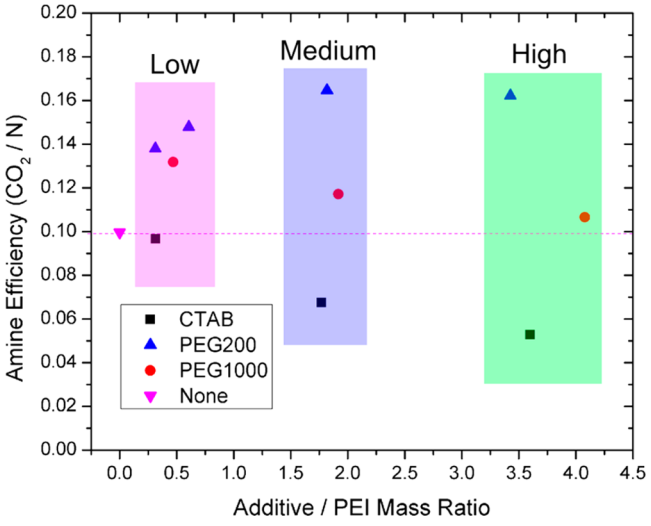

Figure 2. Amine efficiency as a function of additive/PEI mass ratio for CTAB, PEG200, and PEG1000 coincorporated with PEI into SBA-15. Horizontal line represents amine efficiency for PEI/SBA-15 without additive. The PEI/SiO_2 mass ratio was held constant at ~0.45 for all samples.

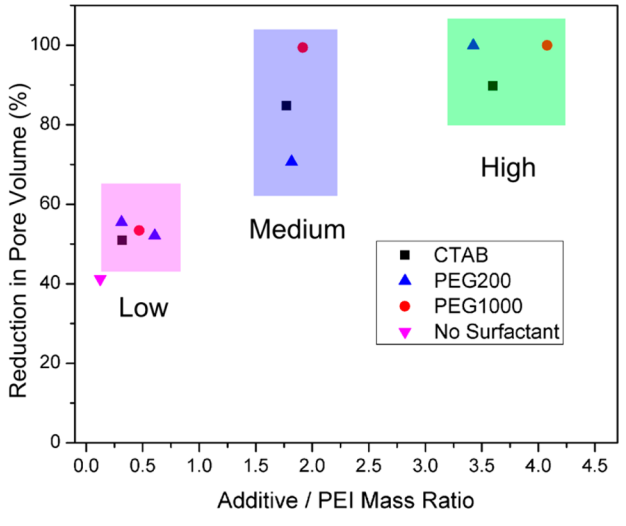

Figure 3. Percentage of pore volume filled by organic as a function of estimated additive/PEI mass ratios for CTAB, PEG1000, and PEG200 incorporated samples.

Samples are grouped by common additive/PEI content, as with Figure 2.

The percentage of pore volume filled or blocked by organic increased with the addition of additive for each set of materials. At additive/PEI ratios of ~0.5 g/g, the pore volumes of the adsorbents were very similar, with just over 50% of the pore volume filled. Similarly, at the highest additive/PEI content the pores of the SBA-15 were nearly full or blocked for each sample set, though the reduction in pore volume of the CTAB sample was slightly less than the others. At the intermediate ~2 g/g additive/PEI content there were stark differences in the reduction in pore volume. The physisorption profiles of the samples at this composition, normalized per gram SiO_2, are shown in Figure 4.

The PEI/PEG200 and PEI/CTAB samples retained the characteristic SBA-15 isotherm shape with shifted hysteresis regions, indicating effective reductions in pore size relative to the bare SBA-15 in both cases. The PEI/PEG1000 sample adsorbed negligible amounts of N_2 and was effectively nonporous. Importantly, the mass content of organic in the materials in Figure 4 were all within 10% of each other, as indicated in Table 1, and differences in the bulk density of the

DOI: 10.1021/acsami.5b07545
ACS Appl. Mater. Interfaces 2015, 7, 24748−24759

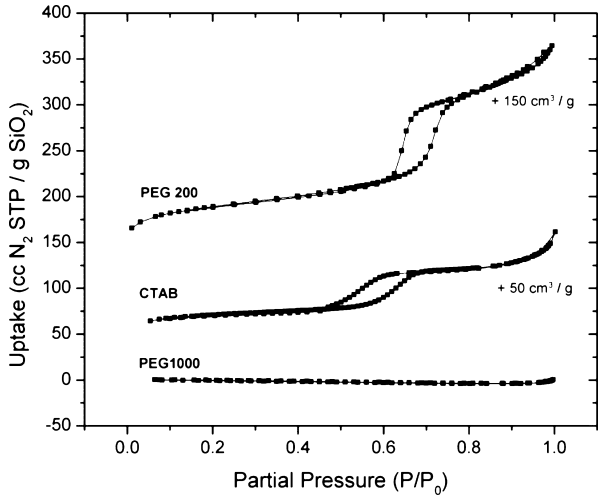

Figure 4. N_2 physisorption profiles for PEI and PEG200 (top), CTAB (middle), and PEG1000 (bottom) coincorporated SBA-15 samples prepared at additive/PEI mass ratios of ~2 (medium additive loading).

different organic mixtures were too small to account for the observed differences in pore volume (Figure S3, Supporting Information). Due to the large quantity of organic contained in the sample, the expected occupied volume of organic exceeded the pore volume of the bare SBA-15 for each of the samples shown in Figure 4, suggesting that there may have been some appreciable organic deposition on the external surface of the particles.

To further investigate this possibility, XPS spectra of the samples at the medium additive loading were measured, as well as for the reference PEI/SBA-15 with no additive. For SBA-15 particles, which are expected to be ~500−1000 nm in diameter,[60] XPS provides a good representation of the surface, probing only a few nanometers deep. Table 2 shows various

Table 2. Molar Ratios Derived from XPS Spectra and Elemental Analysis for Samples with Medium Additive Loading

	SBA/PEI (mol/mol)	SBA/PEI/CTAB (mol/mol)	SBA/PEI/PEG200 (mol/mol)	SBA/PEI/PEG1000 (mol/mol)
C/Si	1.1	2.3	1.5	3.0
O/Si	1.7	1.7	2.0	2.5
N/Si	0.5	0.4	0.4	0.5
C/N	2.3	6.6	3.8	6.0
C/N (EA)	2.3	5.7	5.6	5.8

molar ratios derived from the XPS measurements, along with the bulk C/N molar ratio obtained from elemental analysis for comparison. The raw XPS spectra are provided in Figure S4 of the Supporting Information.

The C/Si ratios of the samples containing additive were each higher than that of the reference PEI/SBA-15, indicating an enhanced degree of organic deposition on the outer surface of the particles. The C/Si ratios followed a similar trend as the reduction in pore volume shown in Figure 3, and the PEI/PEG1000 sample has the greatest amount of organic on the surface, followed by PEI/CTAB and finally PEI/PEG200. O/Si ratios were higher in both PEI/PEG samples than the SBA/PEI control, providing a signature of PEG on the particle exterior of these samples. The surface N/Si ratios were similar for all the samples, suggesting that the amount of PEI deposited on the exterior of the particle did not significantly change during the preparation with or without additive. However, N and Si had the weakest signal in the spectra and, thus, may have the highest intrinsic error associated with integration of the peaks.

The bulk C/N was very similar for each sample while the surface C/N varied between samples. For the control PEI/SBA-15 sample, the C/N ratio measured by both techniques was identical, providing merit for the use of this comparison in distinguishing physical differences within a single material. The most striking difference between surface and bulk C/N was that of the PEI/PEG200, where the surface C/N was significantly lower than the bulk but still higher than that of the PEI/SBA-15 control. This indicates that there was some PEG on the exterior of the particle, consistent with the C/Si and O/Si data, but to a lesser degree than in the bulk. Thus, much of the PEG200 likely went inside the pores of the SBA-15 along with the PEI. Taken together with the TGA, N_2 physisorption and bulk density data, which suggest that this sample contained enough organic to completely fill the pores but retained significant porosity, we hypothesize that the PEI and PEG may have packed in the pores in such a way that the confinement induced a difference in the density of the mixture relative to the bulk (unconfined).

The PEI/PEG1000 had comparable surface and bulk C/N content, indicating that either all of the organic was deposited on the surface, or there was a distribution of homogeneously mixed organic in the interior and exterior of the particles. The significant C and O content on the exterior of the particle coupled with the physisorption data showing no porosity suggests a disproportionate deposition of organic on the exterior of the particle. The PEI/CTAB had a higher surface C/N than bulk, indicating a higher content of CTAB on the particle exterior, consistent with the increased C/Si surface ratio.

The efficient filling of pores is expected to be an important practical consideration in the scale up of adsorbents to structured contactors of hierarchical pore structure such as hollow fibers.[42,61] As such, these findings of heterogeneities in the deposition of polyamine/additive mixtures onto porous particles is an important development, and to our knowledge such have not been previously identified in the literature.

At a more fundamental level, we hypothesize that the observed differences in organic deposition and pore filling derive from additive/PEI molecular interactions. Specifically, through clusters formed between PEG and PEI, but not CTAB and PEI, due to hydrogen bonding interactions. PEG and PEI likely hydrogen bond primarily through interactions between the alcohol end groups on the PEG and primary and secondary amines on the PEI. CTAB likely does not interact as well with the PEI due to the lack of H bonding sites. PEG/PEI clusters would contain multiple PEG chains per PEI chain as a single PEI chain contains ~22 N groups, 75% of which are primary or secondary,[62,63] while PEG contains two alcohol groups. Thus, clusters of PEI/PEG1000 would be larger in radius than PEI/PEG200 and would be more susceptible to blocking SBA-15 mesopores during the solvent removal step of the synthesis, where capillary forces likely play a role in forcefully drawing solution into the pores of the solid. We hypothesize that this is what causes the pore blockage observed in N_2 physisorption of the PEI/PEG1000 sample. Smaller clusters of PEG200 and PEI could have the opposite effect, promoting pore filling, by reducing the interaction between amine groups on the PEI and

DOI: 10.1021/acsami.5b07545
ACS Appl. Mater. Interfaces 2015, 7, 24748−24759

hydroxyls on the pore surface of the silica, thus allowing PEI to settle in a dispersed configuration.

Effect of PEI Loading on Amine Efficiency in SBA-15. To further explore the promoting effect of PEG200 on supported PEI, we co-impregnated SBA-15 with PEG200 at two additional PEI/SiO_2 ratios. Figure 5 shows the amine efficiencies as a function of the PEG/SiO_2 quantity for each PEI loading. Table S1 in the Supporting Information presents the relevant data in tabulated form for these samples.

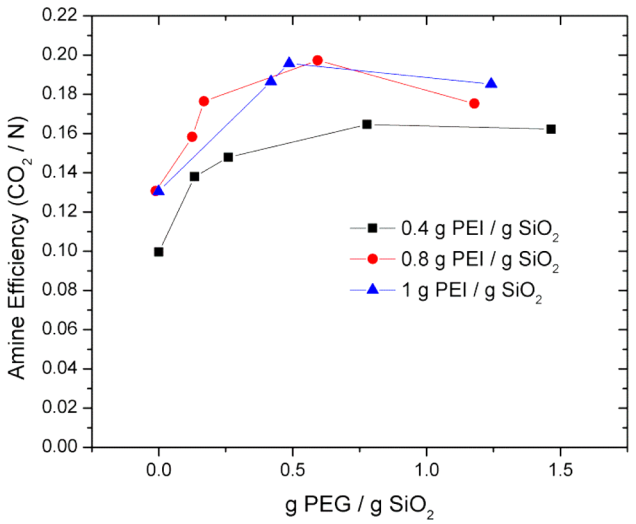

Figure 5. Amine efficiency of PEI co-impregnated with PEG200 at varying PEG200 loadings at three PEI/SiO_2 loadings plotted against estimated PEG/SiO_2 mass ratios estimated from eq 1 and TGA estimations of total organic loading.

The promoting effect of PEG on the amine efficiency was not strongly influenced by the quantity of PEI in the sample, as the shapes of the curves were very similar for each of the PEI loadings tested. The sample data at the two higher PEI loadings were essentially overlapping and shifted a constant value above that for the lowest amine loading. Amine efficiencies are known to increase with amine loading before reaching a plateau, and recent literature suggests that this may be derived from a decreased contribution of amines that interact with the silica wall, which are less active toward CO_2 than amines in the center of the pore.[64] This suggests that the relative amount of PEI on the wall and in the bulk may have been similar for each of the samples upon the addition of PEG and that the PEG primarily altered the amine efficiency of the PEI in the bulk. For each of the three PEI loadings, the relative increase from minimum to maximum was similar at ~60% of the initial efficiency.

CO_2 Adsorption Dynamics. Fractional uptake (normalized adsorbed amount vs time) plots of CO_2 adsorption onto samples discussed in the preceding sections are shown in Figure 6. These provide a qualitative comparison of the adsorption dynamics independent of the total amount of CO_2 adsorbed. In Figure 6a–c, samples of varying additive type and amount are shown, and the data are grouped by similarity in additive/PEI content. In Figure 6d–f, samples of varying PEI and PEG200

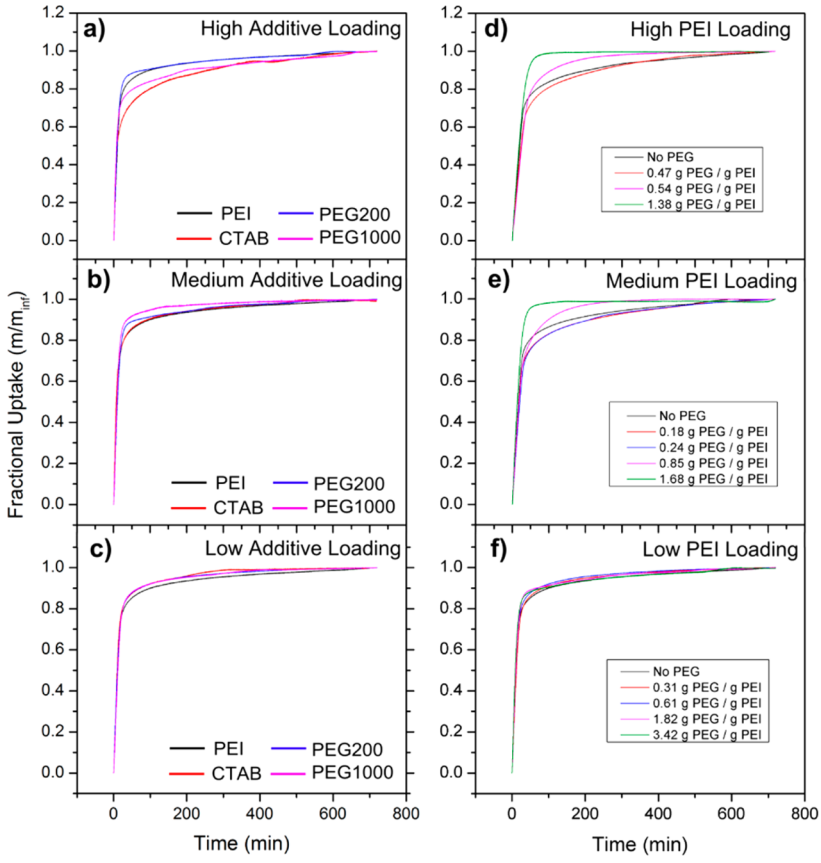

Figure 6. Fractional uptakes of adsorbents prepared (a–c) with varying additive at a single PEI loading and (d–f) with PEI and PEG200 at varying PEI loading.

DOI: 10.1021/acsami.5b07545
ACS Appl. Mater. Interfaces 2015, 7, 24748–24759

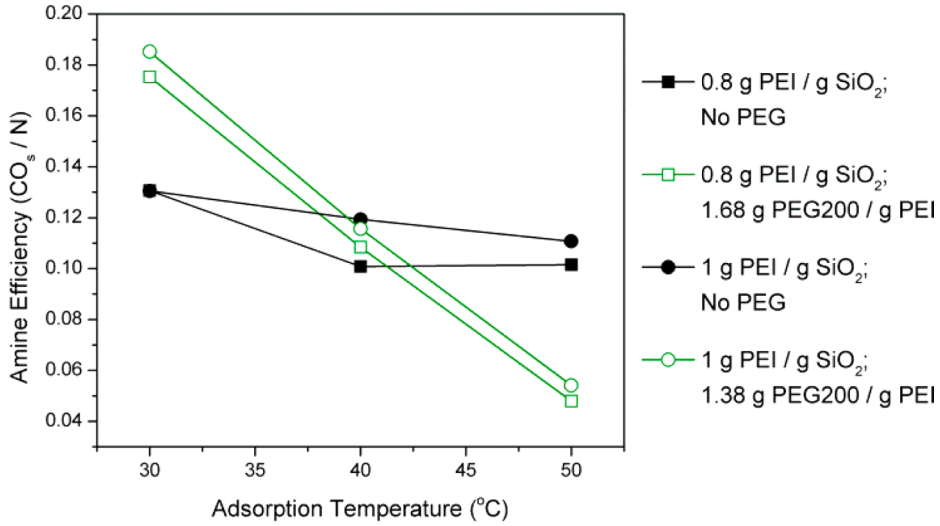

Figure 7. Amine efficiency as a function of adsorption temperature for materials prepared at (■ and □) 0.8 and (● and ○) 1 g PEI/g SiO_2 with PEG200 (green □ and ○) at the highest PEG/SiO_2 loading and (black ■ and ●) without PEG.

content are shown, and the data are grouped by similarity in PEI loading.

The uptakes are characterized by a region of rapid mass uptake at early times of CO_2 exposure, followed by a transition to a slow approach to equilibrium in the long-time region. Such is commonly reported in the literature for supported amines. While a simple model of gas diffusion into a sphere yields a curve with a qualitatively similar shape,[65] the literature suggests that the two regions are the result of multiple regimes of mass transfer resistance.[30] To help interpret this, we reference a recent study characterizing the morphology of PEI inside the pores of SBA-15 as taking the form of a bound monolayer (10–20 wt % PEI) that is less active toward CO_2, and a plug of bulk-like PEI that spans the diameter of the pore but not necessarily the length of the pore, and is more active toward CO_2.[64] With this consideration, the early time, rapid uptake region is hypothesized to result from mass transfer of CO_2 to highly accessible amines in the small bulk PEI domains, perhaps those in close proximity to the interface between the plug and the void in the pores. In the long-time region, there is a slow approach to equilibrium that has been suggested to result from slow CO_2 diffusion to buried amines deep in the plug,[30] or a from slow diffusion due to interamine cross-linking as a result of adsorbed CO_2,[66,67] which would rigidify the PEI and create a physical barrier. Additionally, the bound amines in the monolayer may interact with CO_2 at a different rate than those in the bulk plug, due to crowding of polymers near the silica surface or interaction with the surface hydroxyl groups.

The fractional uptake curves were mostly similar at the low and medium additive loadings as shown in Figure 6b,c with the exception of the PEG1000 sample in Figure 6b, which deviated from the initial rapid uptake region at a slightly higher fractional uptake than the other samples, suggesting that of the amines available for adsorption, were more readily accessible. The amine efficiencies of the PEG200 and PEG1000 incorporated samples (Figure 2) were improved, and the uptake curves suggest that the changes in amine efficiency were manifested at very early times of CO_2 adsorption, perhaps a result of redistributing PEI from a plug to smaller agglomerates. At the higher additive loading, the samples containing CTAB and PEG1000 showed a deviation from the initial region of rapid mass uptake at a lower fractional uptake (y axis value), than the PEG200 and PEI counterparts, reflecting a diminished kinetic performance. In Figure 6d–f, the effect of PEG200 on the uptake dynamics at varying PEI loading is shown. At the low PEI loading, the uptake curves were nearly identical, while the dynamics showed a marked improvement at the two higher PEI loadings and high PEG content. In both cases, at the highest PEG/PEI content the slow approach to equilibrium in the long-time region was not observed. At this particular composition, the content of alcohol end groups of impregnated PEG approached the content of reactive (1° and 2°) amines of PEI (75% of total N),[62,63] taking values of 0.61 and 0.75 mol OH/mol total N for high and medium PEI loadings.

Considering literature precedent[39] that the physical origin of the promoting nature of PEG may be related to OH/N interactions, the hypothesized PEI/PEG cluster formation discussed in the preceding section is extended and discussed in the context of the adsorption behavior. At lower PEG/PEI content, PEG may primarily serve to disperse bulk PEI to smaller agglomerates, resulting in increased amine efficiencies without drastically changed dynamics. At higher PEG/PEI contents, as PEG effectively solvates the PEI, PEG molecules may physically shield PEI chains from one another to reduce individual PEI/PEI chain interactions. This physical shielding of neighboring PEI chains from one another is likely to promote intrachain CO_2 adsorption events (rather than interchain) and would reduce the extent of CO_2 induced PEI cross-linking and the resulting barrier formation and associated diffusional limitations. At the medium and high PEI loadings, a high fraction of PEI is in the bulk, and so a high fraction of CO_2 adsorbs onto PEI in the bulk, and the kinetic effect is clearly observed at high PEG/PEI loadings. At the lower PEI loading, where a higher fraction of PEI is adsorbed to the silica surface (relative to the medium and high PEI samples), is hypothesized that a larger contribution of uptake results from CO_2 adsorption on PEI near the walls. There is evidence, albeit limited, that adsorption of CO_2 onto PEI on the silica walls may be slower than PEI in the bulk, though the physical underpinning is unclear.[64] We emphasize that while this hypothesis is consistent with our data and the literature, a detailed spectroscopic investigation will ultimately be required

DOI: 10.1021/acsami.5b07545
ACS Appl. Mater. Interfaces 2015, 7, 24748–24759

to provide additional evidence to support or refute this hypothesis.

Both molecular weights of PEG may interact with PEI to improve performance in this fashion, but the effect is subject to the clusters being able to efficiently enter the pores of the material. Our data is consistent with this, where at low loadings of PEG1000, where the hypothesized PEG/PEI clusters would have a lower PEG/PEI chain ratio and therefore be smaller, the clusters are more likely to efficiently enter the SBA-15 pores and an improved CO_2 capacity and amine efficiency are observed. However, as the PEG content is increased and the clusters grow in size, clogging at pore mouths occurs and more amines become buried and thus are not available for CO_2 adsorption, even at long adsorption times. Because CTAB likely would not have such interactions with PEI and deposits on the particle exterior disproportionally, it simply may completely block pores at their entrance and bury the impregnated amines at moderate loadings, thus reducing the amine efficiency without significantly altering the dynamics. The relative size of PEG/PEI clusters and pore diameter of the support thus becomes an important metric for future studies.

An alternate hypothesis worth consideration is that the improvement in adsorption dynamics resulted from an increase in the contribution of amines on the particle exterior as opposed to inside the pores, as there was a significant organic content in these highly loaded materials. However, the amine efficiencies of these samples remained high, necessitating that the PEI on the exterior of the particles would either have an exceptionally high efficiency or that PEI molecules have rapid mobility through the pores to the surface such as to rapidly expose a large quantity of unreacted amines.

To further investigate the kinetic behavior, the amine efficiencies of the samples showing the most marked kinetic improvement (1.38 g PEG/g PEI, "High PEI" loading and 1.68 g PEG/g PEI, "Medium PEI" loading) were measured at 40 and 50 °C and compared with the amine efficiencies of the sorbents without PEG. The results of these experiments are shown in Figure 7.

The amine efficiencies decreased at increased adsorption temperature for each sample; however the samples with PEG showed much sharper reductions in amine efficiency at increased temperature than those without PEG. Typically, amine efficiencies of PEI impregnated aminosilica adsorbents show a maximum value at temperatures above 30 °C at higher partial pressures of CO_2, reflecting kinetically controlled systems during the lower temperature experiments.[68] The results in Figure 7 suggest that these kinetic effects may be less important under ultradilute adsorption conditions, where only the most reactive amines will be active, compared to more typical experiments done under higher partial pressures of CO_2 (0.1−1 bar). The steep decrease in capacity of the PEG/PEI samples relative to the samples without PEG indicate a system that is strongly controlled by thermodynamics, thus corroborating the above finding that the adsorption is completely thermodynamically controlled at PEG/PEI ratios approaching equimolar OH/(1°, 2°) N ratios.

Incorporation of PEI and PEG200 in Mesoporous γ-Alumina. Finally, while SBA-15 silica was a useful model for probing adsorption phenomena due to its well-structured nature, such a silica support may not be practical for use in a commercial process. We have previously demonstrated that steam stripping is a potentially practical method for the regeneration of supported amine materials, and that mesoporous alumina is more robust than silica to the conditions imposed by such a process.[55,69−71] While others have suggested that certain silica compositions may also be hydrothermally stable,[72] it is important to explicitly extrapolate the findings of the PEG/PEI/SBA-15 system to other oxides that could be employed as adsorbent supports. As such, the use of PEG as an additive in two γ-alumina supported materials was also explored. One alumina was prepared in house using a soft template (P123), referred to here as "templated" alumina, while the other was a commercially available Sasol Sba-200 alumina referred to here as "commercial alumina". The physisorption profiles, pore size distributions and XRD patterns of the alumina supports are provided in Figures S5 and S6 of the Supporting Information, while the physical and textural properties of the samples derived from such experiments are tabulated in Table S2 in the Supporting Information. Figure 8 shows the amine efficiency of the adsorbents plotted as a function of the PEG/PEI ratio for adsorbents prepared at ∼0.45 g PEI/g support (analogous to Figure 2) as well as that of the SBA-15 materials prepared at the same PEI/SiO_2 loading, for comparison.

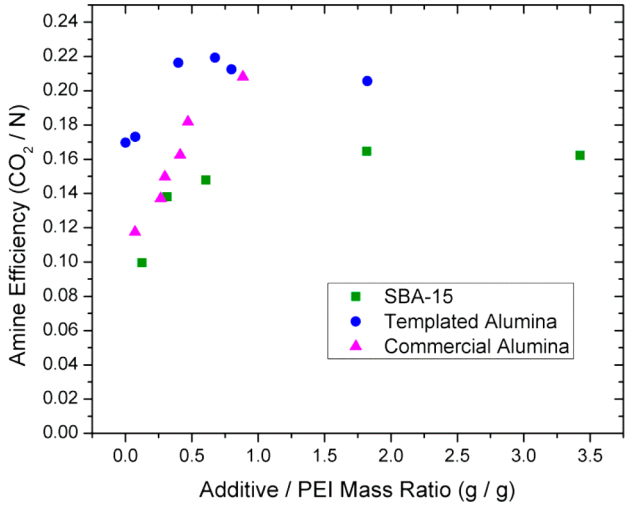

Figure 8. Amine efficiency plotted as a function of PEG200/PEI mass ratio as estimated from eq 1 for (green) SBA-15, (blue) templated alumina, and (magenta) commercial alumina.

Amine efficiencies of the samples without additive differed between supports used, perhaps due to differences in the textural or acid/base properties of the parent support material. The PEI/SBA-15 had an efficiency of ∼0.10, the PEI/commercial alumina was slightly higher at ∼0.12, and the PEI/templated alumina was significantly higher at ∼0.17 mol CO_2/mol N. The pore size of the supports followed the same trend from small to large, suggesting that for these materials, pore size is an important textural property. The acid/base properties likely differed between the supports as well, with the SBA-15 having mild acidity derived from the surface hydroxyls, while the commercial alumina has been shown to have mild acidity,[73,74] and the templated alumina has been shown to have a basic surface.[57] Each material showed the expected increase in amine efficiency with increased PEG200 quantity. The templated alumina reached a maximum before decreasing, while the commercial alumina did not show a maximum. We attempted to incorporate a higher quantity of PEG into this alumina at the given PEI content, but the attempts were

DOI: 10.1021/acsami.5b07545
ACS Appl. Mater. Interfaces 2015, 7, 24748−24759

unsuccessful, likely due to the much lower pore volume of that support compared to the others used (~0.45 vs 1 cm^3/g). The relative increases in amine efficiency at given a PEG content were different between each of the supports. This is in contrast to the data in Figure 7, where the relative increases were very similar for a single support (SBA-15) at varied PEI content, suggesting an interplay between the textural properties of the support and the extent to which PEG alters the adsorption behavior. The textural properties of a support can influence the adsorption behavior of impregnated PEI, where supports of larger pore size, higher pore volume, and a higher degree of pore interconnectivity generally lead to improved performance. However, it remains unclear what the specific physical underpinnings are for these phenomena. The role of surface area is less straightforward, as the model of wall-bound PEI having reduced performance, discussed above, suggests that materials with reduced surface areas lead to higher performing adsorbents. This is consistent with the varied supports here, where the lower surface area aluminas have higher amine efficiencies than the higher surface area silica. The merging of two complex problems, how varied support properties and the addition of PEG alter the adsorption behavior, each without well understood underlying physical mechanisms, is clearly both complicated and important and will require careful future consideration. Nonetheless, these data explicitly demonstrate that the addition of PEG200 to PEI is effective in improving the amine efficiency of PEI supported in alumina, which is important for the further development and engineering of practical materials for CO_2 capture.

CONCLUSIONS

Additive molecules, particularly low molecular weight PEG, PEG200, substantially increased the amine efficiency of PEI supported on mesoporous silica and alumina adsorbing CO_2 from dry simulated air. Amine efficiencies were increased by a maximum of ~60% for each of the PEI loadings tested on SBA-15 silica. At these high PEG/PEI ratios, the materials contain a significant organic content that would result in an increased heating demand during a temperature swing adsorption process. The use of PEG with PEI thus represents a method of tuning the performance of the adsorbent toward reduced capital costs (via increased amine efficiency), at the expense of potentially increased operating cost. A threshold PEG/PEI ratio was identified, at which the adsorption was completely thermodynamically controlled, and which corresponded to equimolar OH/reactive (1°, 2°) amine ratios, providing the means to hypothesize a physical origin of the behavior. It is suggested that PEG and PEI cluster together to reduce PEI/PEI and PEI/SiO_2 that lead to a higher probability of intrachain CO_2 adsorption events, thus reducing the extent of CO_2-induced PEI cross-linking. A nonhomogenous deposition of organic on the interior/exterior of the SBA-15 particles is observed, with the larger molecules (PEG1000, CTAB) preferentially depositing on the particle exterior; thus the PEG/PEI promoting effect is subject to efficient organic incorporation into the support pores. Finally, the use of PEG200 was explicitly demonstrated to be effective in improving the amine efficiency of PEI when supported on mesoporous alumina, a more robust support for practical applications.

ASSOCIATED CONTENT

Supporting Information

The Supporting Information is available free of charge on the ACS Publications website at DOI: 10.1021/acsami.5b07545.

Review of additive use in supported amine materials, FTIR spectra, bulk density of additive/PEI mixtures, raw XPS spectra, properties of PEG200/PEI/SBA-15 adsorbents, characterization of alumina supports, and properties of PEG200/PEI/alumina adsorbents. (PDF)

AUTHOR INFORMATION

Corresponding Author

* Email: cjones@chbe.gatech.edu.

Author Contributions

The manuscript was written through contributions of all authors. All authors have given approval to the final version of the manuscript.

Funding

Research was supported as part of the UNCAGE-ME Center, an Energy Frontier Research Center funded by the U.S. Department of Energy (DOE), Office of Science, Basic Energy Sciences (BES), under Award No. DE-SC0012577 (Pore filling and support effect studies), and by Corning, Inc. (CO_2 adsorption studies).

Notes

The authors declare no competing financial interest.

REFERENCES

(1) Chu, S.; Majumdar, A. Opportunities and Challenges for a Sustainable Energy Future. *Nature* **2012**, *488*, 294−303.

(2) Friedlingstein, P.; Andrew, R. M.; Rogelj, J.; Peters, G. P.; Canadell, J. G.; Knutti, R.; Luderer, G.; Raupach, M. R.; Schaeffer, M.; van Vuuren, D. P.; et al. Persistent Growth of CO_2 Emissions and Implications for Reaching Climate Targets. *Nat. Geosci.* **2014**, *7*, 709−715.

(3) IPCC, 2014: Summary for Policymakers. In *Climate Change 2014: Mitigation of Climate Change. Contribution of Working Group III to the Fifth Assessment Report of the Intergovernmental Panel on Climate Change*. Edenhofer, O., R. Pichs-Madruga, Sokona, Y.; Farahani, E.; Kadner, S.; Seyboth, K.; Adler, A.; Baum, I.; Brunner, S.; Eickemeier, P.; Kriemann, B.; Savolainen, J.; S. Schlömer, C. von Stechow, Zwickel, T.; and Minx, J. C. Eds.; Cambridge University Press: Cambridge, United Kingdom.

(4) Haszeldine, R. S. Carbon Capture and Storage: How Green Can Black Be? *Science* **2009**, *325*, 1647−1652.

(5) D'Alessandro, D. M.; Smit, B.; Long, J. R. Carbon Dioxide Capture: Prospects for New Materials. *Angew. Chem., Int. Ed.* **2010**, *49*, 6058−6082.

(6) Boot-Handford, M. E.; Abanades, J. C.; Anthony, E. J.; Blunt, M. J.; Brandani, S.; Mac Dowell, N.; Fernández, J. R.; Ferrari, M.-C.; Gross, R.; Hallett, J. P.; Haszeldine, R. S.; Heptonstall, P.; Lyngfelt, A.; Makuch, Z.; Mangano, E.; Porter, R. T. J.; Pourkashanian, M.; Rochelle, G. T.; Shah, N.; Yao, J. G.; Fennell, P. S. Carbon Capture and Storage Update. *Energy Environ. Sci.* **2014**, *7*, 130−189.

(7) Goeppert, A.; Czaun, M.; Surya Prakash, G. K.; Olah, G. A. Air as the Renewable Carbon Source of the Future: An Overview of CO_2 Capture from the Atmosphere. *Energy Environ. Sci.* **2012**, *5*, 7833−7853.

(8) Jones, C. W. CO_2 Capture from Dilute Gases as a Component of Modern Global Carbon Management. *Annu. Rev. Chem. Biomol. Eng.* **2011**, *2*, 31−52.

(9) Keith, D. W. Why Capture CO_2 from the Atmosphere? *Science* **2009**, *325*, 1654−1655.

(10) Lackner, K. S. Capture of Carbon Dioxide from Ambient Air. *Eur. Phys. J.: Spec. Top.* **2009**, *176*, 93−106.

DOI: 10.1021/acsami.5b07545
ACS Appl. Mater. Interfaces 2015, 7, 24748−24759

(11) Tavoni, M.; Socolow, R. Modeling Meets Science and Technology: An Introduction to a Special Issue on Negative Emissions. *Clim. Change* **2013**, *118*, 1−14.
(12) Lackner, K. S.; Brennan, S.; Matter, J. M.; Park, A-H.; Wright, A.; van der Zwaan, B. The Urgency of the Development of CO_2 Capture from Ambient Air. *Proc. Natl. Acad. Sci. U. S. A.* **2012**, *109*, 13156−13162.
(13) Socolow, R.; Desmond, M.; Aines, R.; Blackstock, J.; Bolland, O.; Kaarsberg, T.; Lewis, N.; Mazzotti, M.; Pfeffer, A.; Sawyer, K.; Siirola, J.; Smit, B.; Wilcox, J. *Direct Air Capture of CO_2 with Chemicals: A Technology Assessment for the APS Panel on Public Affairs*. American Physical Society: College Park, MD, 2011.
(14) Bollini, P.; Didas, S. A.; Jones, C. W. Amine-Oxide Hybrid Materials for Acid Gas Separations. *J. Mater. Chem.* **2011**, *21*, 15100−15120.
(15) Choi, S.; Drese, J. H.; Jones, C. W. Adsorbent Materials for Carbon Dioxide Capture from Large Anthropogenic Point Sources. *ChemSusChem* **2009**, *2*, 796−854.
(16) Drage, T. C.; Snape, C. E.; Stevens, L. A.; Wood, J.; Wang, J.; Cooper, A. I.; Dawson, R.; Guo, X.; Satterley, C.; Irons, R. Materials Challenges for the Development of Solid Sorbents for Post-Combustion Carbon Capture. *J. Mater. Chem.* **2012**, *22*, 2815−2823.
(17) Alkhabbaz, M. A.; Bollini, P.; Foo, G. S.; Sievers, C.; Jones, C. W. Important Roles of Enthalpic and Entropic Contributions to CO_2 Capture from Simulated Flue Gas and Ambient Air Using Mesoporous Silica Grafted Amines. *J. Am. Chem. Soc.* **2014**, *136*, 13170−13173.
(18) Didas, S. A.; Kulkarni, A. R.; Sholl, D. S.; Jones, C. W. Role of Amine Structure on Carbon Dioxide Adsorption from Ultradilute Gas Streams such as Ambient Air. *ChemSusChem* **2012**, *5*, 2058−2064.
(19) Wurzbacher, J. A.; Gebald, C.; Steinfeld, A. Separation of CO_2 from Air by Temperature-Vacuum Swing Adsorption Using Diamine-Functionalized Silica Gel. *Energy Environ. Sci.* **2011**, *4*, 3584−3592.
(20) Choi, S.; Drese, J. H.; Eisenberger, P. M.; Jones, C. W. Application of Amine-Tethered Solid Sorbents for Direct CO_2 Capture from the Ambient Air. *Environ. Sci. Technol.* **2011**, *45*, 2420−2427.
(21) Belmabkhout, Y.; Serna-Guerrero, R.; Sayari, A. Amine-Bearing Mesoporous Silica for CO_2 Removal from Dry and Humid Air. *Chem. Eng. Sci.* **2010**, *65*, 3695−3698.
(22) Stuckert, N. R.; Yang, R. T. CO_2 Capture from the Atmosphere and Simultaneous Concentration Using Zeolites and Amine-Grafted SBA-15. *Environ. Sci. Technol.* **2011**, *45*, 10257−10264.
(23) Chichilnisky, G.; Eisenberger, P. M. System and Method for Removing Carbon Dioxide from an Atmosphere and Global Thermostat Using the Same. U.S. Patent 20080289495A1, Nov. 27, 2008.
(24) Eisenberger, P. Carbon Dioxide Capture/Regneration Method Using Monolith U.S. Patent 20120167764A1, July 5, 2012.
(25) Kulkarni, A. R.; Sholl, D. S. Analysis of Equilibrium-Based TSA Processes for Direct Capture of CO2 from Air. *Ind. Eng. Chem. Res.* **2012**, *51*, 8631−8645.
(26) Donaldson, T. L.; Nguyen, Y. N. Carbon Dioxide Reaction Kinetics and Transport in Aqueous Amine Membranes. *Ind. Eng. Chem. Fundam.* **1980**, *19*, 260−266.
(27) Aziz, B.; Hedin, N.; Bacsik, Z. Quantification of Chemisorption and Physisorption of Carbon Dioxide on Porous Silica Modified by Propylamines: Effect of Amine Density. *Microporous Mesoporous Mater.* **2012**, *159*, 42−49.
(28) Harlick, P. J. E.; Sayari, A. Applications of Pore-Expanded Mesoporous Silica 5. Triamine Grafted Material with Exceptional CO_2 Dynamic and Equilibrium Adsorption Performance. *Ind. Eng. Chem. Res.* **2007**, *46*, 446−458.
(29) Brunelli, N. A.; Didas, S. A.; Venkatasubbaiah, K.; Jones, C. W. Tuning Cooperativity by Controlling the Linker Length of Silica-Supported Amines in Catalysis and CO_2 Capture. *J. Am. Chem. Soc.* **2012**, *134*, 13950−13953.
(30) Bollini, P.; Brunelli, N. A.; Didas, S. A.; Jones, C. W. Dynamics of CO_2 Adsorption on Amine Adsorbents. 2. Insights Into Adsorbent Design. *Ind. Eng. Chem. Res.* **2012**, *51*, 15153−15162.
(31) Wang, J.; Wang, M.; Li, W.; Qiao, W.; Long, D.; Ling, L. Application of Polyethyleneimine-Impregnated Solid Adsorbents for Direct Capture of Low-Concentration CO_2. *AIChE J.* **2015**, *61*, 972−980.
(32) Satyapal, S.; Filburn, T.; Trela, J.; Strange, J. Performance and Properties of a Solid Amine Sorbent for Carbon Dioxide Removal in Space Life Support Applications. *Energy Fuels* **2001**, *15*, 250−255.
(33) Xu, X.; Song, C.; Andrésen, J. M.; Miller, B. G.; Scaroni, A. W. Preparation and Characterization of Novel CO_2 "Molecular Basket" Adsorbents Based on Polymer-Modified Mesoporous Molecular Sieve MCM-41. *Microporous Mesoporous Mater.* **2003**, *62*, 29−45.
(34) Arenillas, A.; Smith, K. M.; Drage, T. C.; Snape, C. E. CO_2 Capture Using Some Fly Ash-Derived Carbon Materials. *Fuel* **2005**, *84*, 2204−2210.
(35) Goeppert, A.; Meth, S.; Prakash, G. K. S.; Olah, G. A. Nanostructured Silica as a Support for Regenerable High-Capacity Organoamine-Based CO_2 Sorbents. *Energy Environ. Sci.* **2010**, *3*, 1949−1960.
(36) Meth, S.; Goeppert, A.; Prakash, G. K. S.; Olah, G. A. Silica Nanoparticles as Supports for Regenerable CO_2 Sorbents. *Energy Fuels* **2012**, *26*, 3082−1090.
(37) Wang, J.; Long, D.; Zhou, H.; Chen, Q.; Liu, X.; Ling, L. Surfactant Promoted Solid Amine Sorbents for CO_2 Capture. *Energy Environ. Sci.* **2012**, *5*, 5742−5749.
(38) Wang, J.; Wang, M.; Zhao, B.; Qiao, W.; Long, D.; Ling, L. Mesoporous Carbon-Supported Solid Amine Sorbents for Low-Temperature Carbon Dioxide Capture. *Ind. Eng. Chem. Res.* **2013**, *52*, 5437−5444.
(39) Tanthana, J.; Chuang, S. S. C. In Situ Infrared Study of the Role of PEG in Stabilizing Silica-Supported Amines for CO_2 Capture. *ChemSusChem* **2010**, *3*, 957−964.
(40) Srikanth, C. S.; Chuang, S. S. C. Spectroscopic Investigation into Oxidative Degradation of Silica-Supported Amine Sorbents for CO_2 Capture. *ChemSusChem* **2012**, *5*, 1435−1442.
(41) Srikanth, C. S.; Chuang, S. S. C. Infrared Study of Strongly and Weakly Adsorbed CO_2 on Fresh and Oxidatively Degraded Amine Sorbents. *J. Phys. Chem. C* **2013**, *117*, 9196−9205.
(42) Labreche, Y.; Fan, Y.; Rezaei, F.; Lively, R. P.; Jones, C. W.; Koros, W. J. Poly(amide-imide)/Silica Supported PEI Hollow Fiber Sorbents for Postcombustion CO_2 Capture by RTSA. *ACS Appl. Mater. Interfaces* **2014**, *6*, 19336−19346.
(43) Wang, J.; Huang, H.; Wang, M.; Yao, L.; Qiao, W.; Long, D.; Ling, L. Direct Capture of Low-Concentration CO_2 on Mesoporous Carbon-Supported Solid Amine Adsorbents at Ambient Temperature. *Ind. Eng. Chem. Res.* **2015**, *54*, 5319−5327.
(44) Heydari-Gorji, A.; Belmabkhout, Y.; Sayari, A. Polyethylenimine-Impregnated Mesoporous Silica: Effect of Amine Loading and Surface Alkyl Chains on CO_2 Adsorption. *Langmuir* **2011**, *27*, 12411−12416.
(45) Heydari-Gorji, A.; Sayari, A. CO_2 Capture on Polyethylenimine-Impregnated Hydrophobic Mesoporous Silica: Experimental and Kinetic Modeling. *Chem. Eng. J.* **2011**, *173*, 72−79.
(46) Yue, M. B.; Chun, Y.; Cao, Y.; Dong, X.; Zhu, J. H. CO_2 Capture by As-Prepared SBA-15 with an Occluded Organic Template. *Adv. Funct. Mater.* **2006**, *16*, 1717−1722.
(47) Fauth, D. J.; Gray, M. L.; Pennline, H. W.; Krutka, H. M.; Sjostrom, S.; Ault, A. M. Investigation of Porous Silica Supported Mixed-Amine Sorbents for Post-Combustion CO_2 Capture. *Energy Fuels* **2012**, *26*, 2483−2496.
(48) Sanz, R.; Calleja, G.; Arencibia, A.; Sanz-Pérez, E. S. CO_2 Uptake and Adsorption Kinetics of Pore-Expanded SBA-15 Double-Functionalized with Amino Groups Rau L. *Energy Fuels* **2013**, *27*, 7637−7644.
(49) Liu, J.; Cheng, D.; Liu, Y.; Wu, Z. Adsorptive Removal of Carbon Dioxide Using Polyethyleneimine Supported on Propane-sulfonic-Acid-Functionalized Mesoporous. *Energy Fuels* **2013**, *27*, 5416−5422.
(50) Sanz, R.; Calleja, G.; Arencibia, A.; Sanz-Pérez, E. S. Development of High Efficiency Adsorbents for CO_2 Capture Based

DOI: 10.1021/acsami.5b07545
ACS Appl. Mater. Interfaces 2015, 7, 24748−24759

on a Double-Functionalization Method of Grafting and Impregnation. *J. Mater. Chem. A* **2013**, *1*, 1956−1962.
(51) Choi, S.; Gray, M. L.; Jones, C. W. Amine-Tethered Solid Adsorbents Coupling High Adsorption Capacity and Regenerability for CO_2 Capture from Ambient Air. *ChemSusChem* **2011**, *4*, 628−635.
(52) Wang, X.; Song, C. New Strategy To Enhance CO_2 Capture over a Nanoporous Polyethylenimine Sorbent. *Energy Fuels* **2014**, *28*, 7742−7745.
(53) Zhu, J.; Baker, S. N. Lewis Base Polymers for Modifying Sorption and Regeneration Abilities of Amine-Based Carbon Dioxide Capture Materials. *ACS Sustainable Chem. Eng.* **2014**, *2*, 2666−2674.
(54) Serna-Guerrero, R.; Belmabkhout, Y.; Sayari, A. Modeling CO_2 Adsorption on Amine-Functionalized Mesoporous Silica: 1. A Semi-Empirical Equilibrium Model. *Chem. Eng. J.* **2010**, *161*, 173−181.
(55) Chaikittisilp, W.; Kim, H.-J.; Jones, C. W. Mesoporous Alumina-Supported Amines as Potential Steam-Stable Adsorbents for Capturing CO_2 from Simulated Flue Gas and Ambient Air. *Energy Fuels* **2011**, *25*, 5528−5537.
(56) Bali, S.; Chen, T. T.; Chaikittisilp, W.; Jones, C. W. Oxidative Stability of Amino Polymer−Alumina Hybrid Adsorbents for Carbon Dioxide Capture. *Energy Fuels* **2013**, *27*, 1547−1554.
(57) Fulvio, P. F.; Brosey, R. I.; Jaroniec, M. Synthesis of Mesoporous Alumina from Boehmite in the Presence of Triblock Copolymer. *ACS Appl. Mater. Interfaces* **2010**, *2*, 588−593.
(58) Zhang, Z.; Pinnavaia, T. J. Mesoporous Gamma-Alumina Formed through the Surfactant-Mediated Scaffolding of Peptized Pseudoboehmite Nanoparticles. *Langmuir* **2010**, *26*, 10063−10067.
(59) Liu, Q.; Wang, A.; Wang, X.; Gao, P.; Wang, X.; Zhang, T. Synthesis, Characterization and Catalytic Applications of Mesoporous Γ-Alumina from Boehmite Sol. *Microporous Mesoporous Mater.* **2008**, *111*, 323−333.
(60) Lee, H. I.; Kim, J. H.; Stucky, G. D.; Shi, Y.; Pak, C.; Kim, J. M. Morphology-Selective Synthesis of Mesoporous SBA-15 Particles over Micrometer, Submicrometer and Nanometer Scales. *J. Mater. Chem.* **2010**, *20*, 8483−8487.
(61) Labreche, Y.; Lively, R. P.; Rezaei, F.; Chen, G.; Jones, C. W.; Koros, W. J. Post-Spinning Infusion of Poly(ethyleneimine) into Polymer/silica Hollow Fiber Sorbents for Carbon Dioxide Capture. *Chem. Eng. J.* **2013**, *221*, 166−175.
(62) Drese, J. H.; Choi, S.; Lively, R. P.; Koros, W. J.; Fauth, D. J.; Gray, M. L.; Jones, C. W. Synthesis-Structure-Property Relationships for Hyperbranched Aminosilica CO_2 Adsorbents. *Adv. Funct. Mater.* **2009**, *19*, 3821−3832.
(63) Von Harpe, A.; Petersen, H.; Li, Y.; Kissel, T. Characterization of Commercially Available and Synthesized Polyethylenimines for Gene Delivery. *J. Controlled Release* **2000**, *69*, 309−322.
(64) Holewinski, A.; Sakwa-Novak, M. A.; Jones, C. W. Linking CO_2 Sorption Performance to Polymer Morphology in Aminopolymer/Silica Composites through Neutron Scattering. *J. Am. Chem. Soc.* **2015**, *137*, 11749−11759.
(65) Ruthven, D. M. *Principles of Adsorption & Adsorption Processes*; John Wiley & Sons: New York, 1984.
(66) Wilfong, W. C.; Chuang, S. S. C. Probing the Adsorption/Desorption of CO_2 on Amine Sorbents by Transient Infrared Studies of Adsorbed CO_2 and C_6H_6. *Ind. Eng. Chem. Res.* **2014**, *53*, 4224−4231.
(67) Wilfong, W. C.; Srikanth, C. S.; Chuang, S. S. C. In Situ ATR and DRIFTS Studies of the Nature of Adsorbed CO_2 on Tetraethylenepentamine Films. *ACS Appl. Mater. Interfaces* **2014**, *6*, 13617−13626.
(68) Xu, X.; Song, C.; Andresen, J. M.; Miller, B. G.; Scaroni, A. W. Novel Polyethylenimine-Modified Mesoporous Molecular Sieve of MCM-41 Type as High-Capacity Adsorbent for CO_2 Capture. *Energy Fuels* **2002**, *16*, 1463−1469.
(69) Sakwa-Novak, M. A.; Jones, C. W. Steam Induced Structural Changes of a Poly(ethylenimine) Impregnated Γ Alumina Sorbent for CO_2 Extraction from Ambient Air. *ACS Appl. Mater. Interfaces* **2014**, *6*, 9245−9255.
(70) Li, W.; Choi, S.; Drese, J. H.; Hornbostel, M.; Krishnan, G.; Eisenberger, P. M.; Jones, C. W. Steam-Stripping for Regeneration of Supported Amine-Based CO_2 Adsorbents. *ChemSusChem* **2010**, *3*, 899−903.
(71) Li, W.; Bollini, P.; Didas, S. A.; Choi, S.; Drese, J. H.; Jones, C. W. Structural Changes of Silica Mesocellular Foam Supported Amine-Functionalized CO_2 Adsorbents upon Exposure to Steam. *ACS Appl. Mater. Interfaces* **2010**, *2*, 3363−3372.
(72) Hammache, S.; Hoffman, J. S.; Gray, M. L.; Fauth, D. J.; Howard, B. H.; Pennline, H. W. Comprehensive Study of the Impact of Steam on Polyethyleneimine on Silica for CO_2 Capture. *Energy Fuels* **2013**, *27*, 6899−6905.
(73) Baca, M.; de la Rochefoucauld, E.; Ambroise, E.; Krafft, J. M.; Hajjar, R.; Man, P. P.; Carrier, X.; Blanchard, J. Characterization of Mesoporous Alumina Prepared by Surface Alumination of SBA-15. *Microporous Mesoporous Mater.* **2008**, *110*, 232−241.
(74) Baca, M.; Carrier, X.; Blanchard, J. Confinement in Nanopores at the Oxide/water Interface: Modification of Alumina Adsorption Properties. *Chem. - Eur. J.* **2008**, *14*, 6142−6148.

DOI: 10.1021/acsami.5b07545
ACS Appl. Mater. Interfaces 2015, 7, 24748−24759